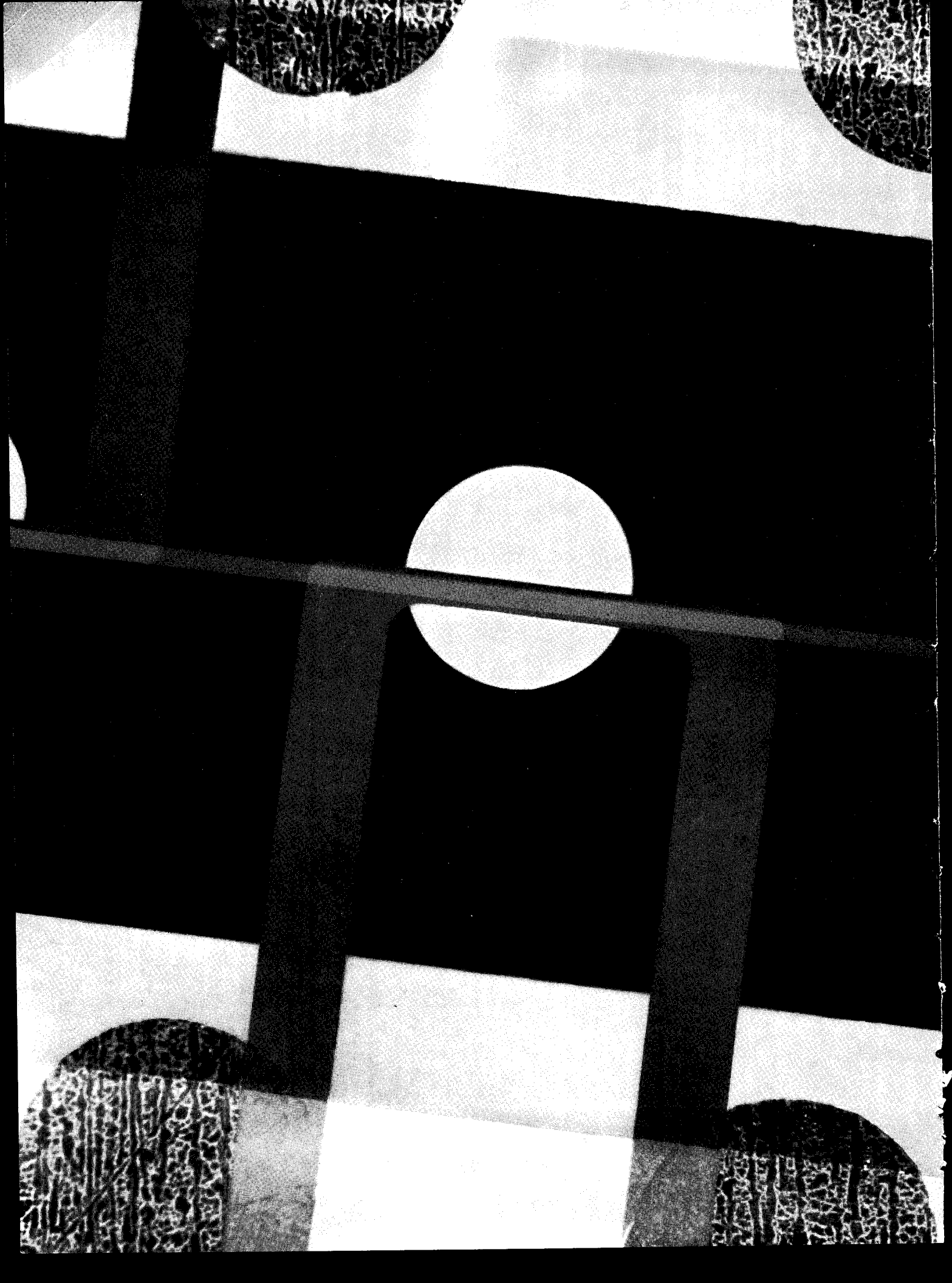

Preface

The intriguing properties of matter which are inherent only at low temperatures led IBM to initiate a low-temperature research program in 1954. The application of some of these properties to circuit components has been recently demonstrated by the use of superconductivity for computer components by D. A. Buck and by the development of the Solid State Maser by Bell Telephone Laboratories.† This work has spearheaded a serious investigation into the possibility of using components that require low temperatures (below 10°K) in circuits of practical interest. Progress in this area has been greatly facilitated by the development of the Collins Cryostat manufactured by the A. D. Little Company. This has made liquid helium readily available to numerous laboratories.*

The use of persistent circulating currents occurring in superconducting materials suggests itself as a means of storing information. The possibility has been investigated by Crowe and Garwin, and the following papers are the first to describe this new work. The results have been most encouraging and have led us to look forward with enthusiasm toward the future possibilities of low-temperature circuitry.

D. R. Young, Manager
IBM Cryogenics Research Department

*D. A. Buck, *Proc. IRE* **44**, 482 (April 1956).
†Scovil, Feher and Seidel, *Phys. Rev.* **105**, 762 (Jan. 15, 1957).

J. W. Crowe

Trapped-Flux Superconducting Memory*

Abstract: A memory cell based on trapped flux in superconductors has been built and tested. The cell is constructed entirely by vacuum evaporation of thin films and can be selected by coincident current or by other techniques, with drive-current requirements less than 150 ma. The short transition time of the trapped-flux cell indicates its possible use in high-speed memories. The superconductive film memory does not exhibit the problems of "delta noise" in core memories resulting from the difference in half-select pulse outputs.

Introduction

The discovery of superconductivity in 1911 by H. Kamerlingh Onnes[1] opened up an entirely new dimension in physical research: investigation of the phenomena of electrical properties at low temperatures. Between 1911 and 1952 the theoretical aspects of superconductivity generally have been studied according to six basic categories: (1) transition to zero resistance; (2) intermediate-state; (3) flux-trapping; (4) flux-exclusion, i.e., Meissner effect; (5) the destruction of the superconductive state by means of a current; and (6) sharpness of threshold. More recently (1953-1956) D. A. Buck's[2] work with the cryotron demonstrated that superconductive metals could be used in flip-flop circuits, gates, counters, and other computer circuitry. In the area of flux-trapping studies, an extension of some previous demonstrations of supercurrents by S. C. Collins[3] at MIT showed that trapped flux could be maintained in a superconducting ring for more than two years.†

Since the work of Buck, Collins and others showed the feasibility of computer components that would respond to the magnetic control of the superconducting and normal states in tantalum, work was started at this laboratory on the study of a high-speed, high-capacity memory based on the principle of trapping flux in a superconduct-

Figure 1 **Superconducting cell showing detail of U-shaped Y drive wire.**

*Presented in part at Conference on Low Temperature Physics, at Madison, Wisc., August 26, 1957. Conference was jointly sponsored by International Union of Applied Physics, American Physical Society and University of Wisconsin.

†No perceptible decay was noticed from March 16, 1954, when the test was initiated, until September 11, 1956, at which time the test was discontinued. In order that no change of flux be detectable the resistance must be less than 10^{-21} ohms, assuming a measurement accuracy of 1%.

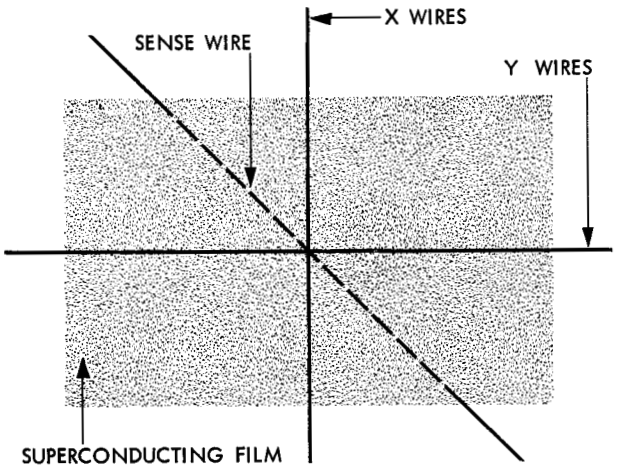

Figure 2 **Early concept of memory cell in which the sense wire would intersect both X and Y wires at 45° angle.**

ing film. For the demonstration and measurement of this phenomenon, a memory cell based on trapped flux in superconductors was built.

The purpose of this paper is to describe a new type of superconducting memory cell utilizing a lead film and to show its operational characteristics. Analyses are made of the relation of the magnetic field to drive-current density and of the time dependence of the penetration of the magnetic field in the memory cell. For purposes of definition, the switching function is interpreted on the basis of destruction of the superconducting state by a critical current density, rather than by a critical field density.[4]

Initial cell geometry

An attempt was first made to draw up a basic design for cell geometry. Our early studies of the phenomenological theory of zero resistance and flux trapping indicated that a memory cell (Fig. 2) could consist essentially of an X-group of horizontal drive wires crossing a Y-group at right angles. A sense wire placed at 45° to the XY junction would intersect all the crossings in the network. The superconducting film was provided in order to trap the flux.

To investigate the superconductive aspects implied in Fig. 2, a laboratory device was constructed according to the configuration shown in Fig. 3. This device was designed with drive coils of several turns to provide a high magnetic field and with the superconducting film to serve as a flux barrier, at low magnetic-field strengths, between the input (pulsed-current drive coil) and the output (sense winding). Tests with this simple configuration did show that the film prevented flux penetration at field strengths below a critical value. At low fields, the flux lines are presumably forced along the surface of the film, inducing circulating currents. When the critical current density is reached, the film is forced into the normal conductive state, which permits flux to penetrate the film and flux lines to link a portion of the film. The induced currents that opposed the field now decay. After removal of the drive current the flux is apparently trapped in cracks and imperfections in the film.[5]

Test memory cell

After the flux-trapping property of the film was established, a test cell was made, in which a hole was provided to serve the function of the imperfections in the film of Fig. 3. In this test memory cell (Fig. 4) there is a "hard" superconducting film,* with a thin crossbar of superconductive material vacuum-metallized across the hole and placed in electrical contact with the film. Although both film and crossbar are made of lead, the crossbar is a "soft" superconductor because it is thinner than the film.†

Driving is accomplished by means of drive wires placed parallel to the crossbar. A sense wire, located beneath the film, detects flux changes. This particular geometry was selected because it provides the features of the laboratory model in a way that is more readily controllable.

The test cell shown in Fig. 4 was intended to trap flux in a doughnut pattern, as shown in Fig. 5. The current flow in Fig. 5a was intended to represent in a binary system a value of "1", and the current direction in Fig. 5b a value of "0".

*The "hard" superconductor, as defined here, is characterized by a high critical field and "soft" superconductor by low critical field.

†Originally a square hole with a thin bar across it was contemplated. There is no operational difference between this and the round hole discussed in this paper.

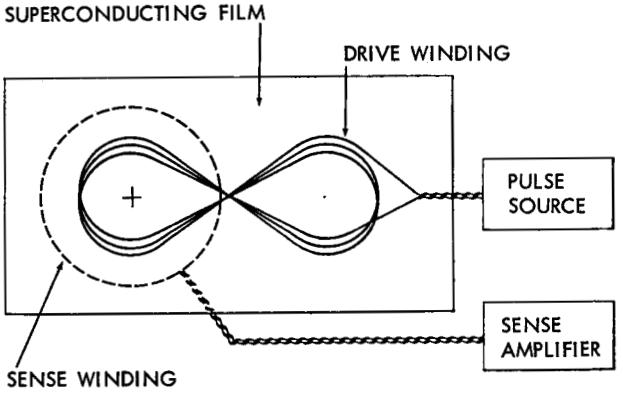

Figure 3 **Experimental superconducting device.** *Pulsed current in two drive windings establishes a closed flux path which penetrates the superconducting film after the critical field is reached. A 40-turn coil is twisted into a "figure 8". The cross within one loop indicates magnetic flux extending into the plane of the film; the dot shows the flux direction out of the film plane.*

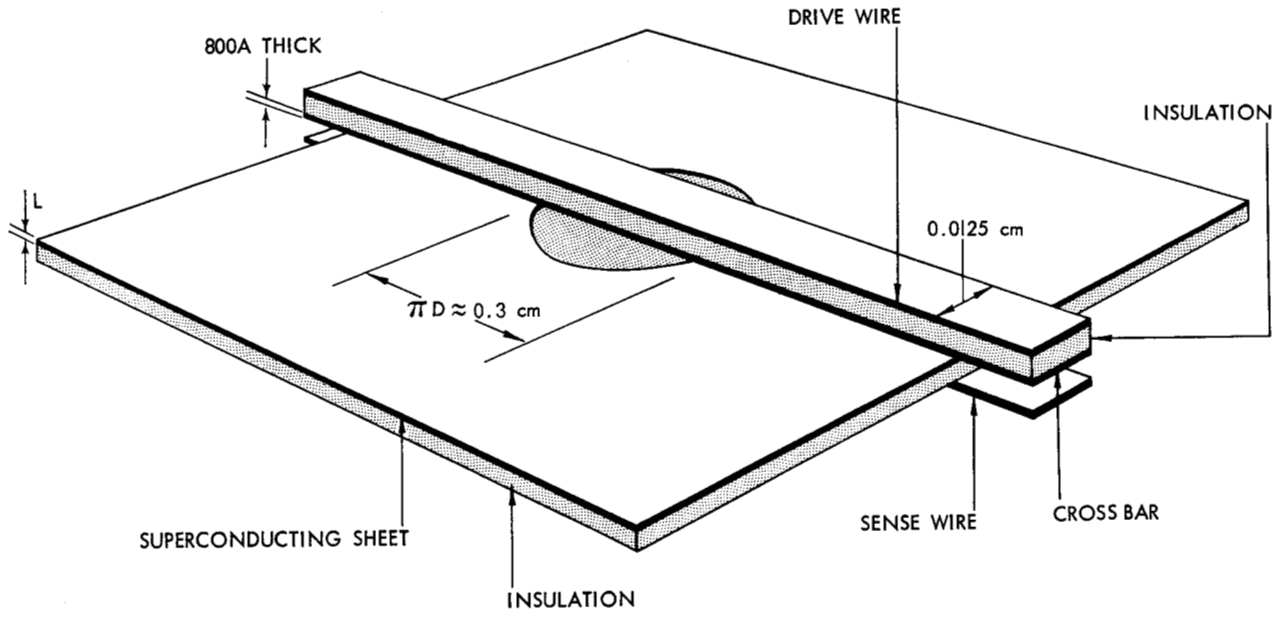

Figure 4 **Test model of memory cell.**
Flux-trapping functions of the imperfections of the film in Fig. 2 are provided by a hole in the superconducting film. ($\pi D \approx 0.3$ cm.) Crossbar = 0.0125 cm wide × 800 A thick.

Figure 5 **Flux-trapping action in holes or imperfections in test cells.**
The dots represent flux lines coming out of the film plane and the crosses, lines going into the plane.

a) Current flow for "one" state. *b) Current flow for "zero" state.*

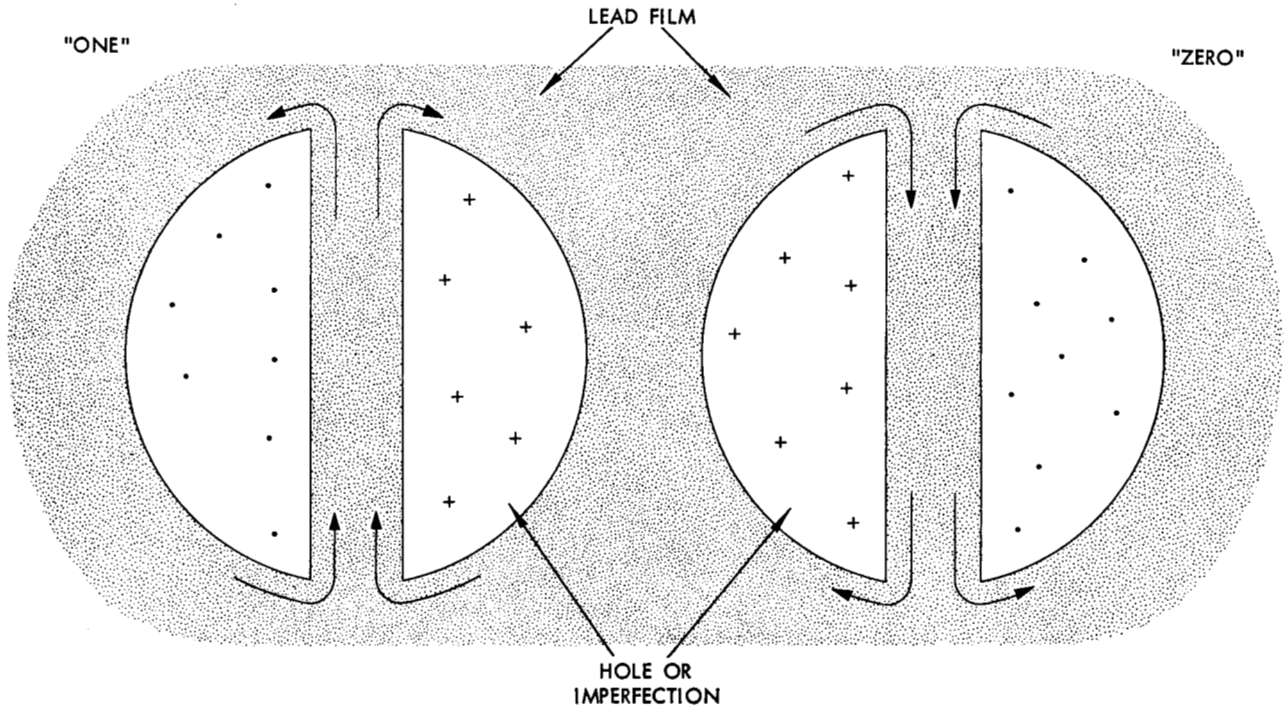

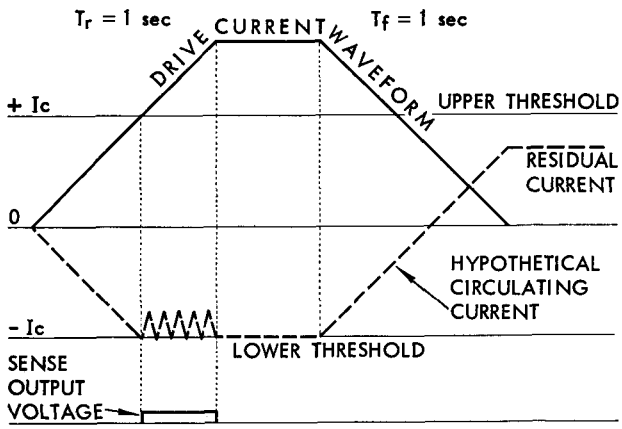

Figure 6a **Characteristic waveforms of test cell.** *Pulse with rise time of 1 sec.*

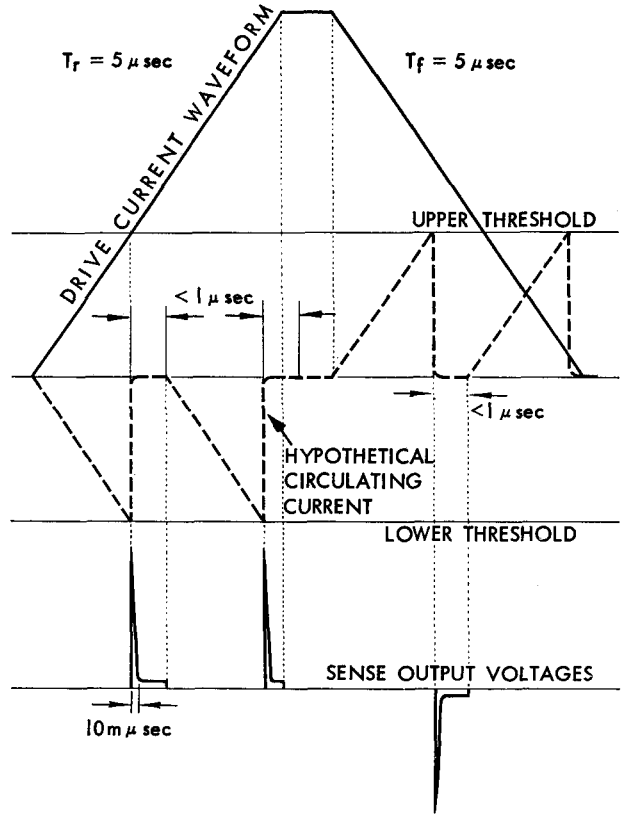

Figure 6b **Characteristic waveforms of test cell.** *Pulse with rise time of 5 μsec.*

Test memory cell: operating characteristics

The operating characteristics of the test memory cell are best described in terms of the oscilloscope waveforms which are approximated by the solid lines in Figs. 6a and 6b. The dashed lines are the hypothetical circulating currents induced in the "soft" crossbar when it is superconducting.

The voltage picked up by the sense wire depends on the rise time of the drive pulse, as indicated in Fig. 6a. *For a very slow rise time* of about one second, we observed that

a) The output voltage at the sense wire is square-shaped and is proportional to the slope of the leading edge of the drive pulse.
b) The output begins when the drive current reaches the upper threshold and ends when this current stops rising.
c) No output is observed during the fall time of the drive-current pulse.

For a fast rise time (about five microseconds) we observed that

a) The sense output is much higher than for slow rise times and very sharply peaked, as shown in Fig. 6b.
b) The threshold for the initiation of the output voltage during the backswing of the drive current in Fig. 6c is a function of pulse width.
c) If the bit has a sharp threshold, a "priming" pulse is necessary in order to start information storage. (Fig. 6d represents a complete memory cycle).

The manner in which cell operation is affected by drive-pulse rise time and duration may be interpreted in the following way. When the memory cell is pulsed at low rise times in the order of one second (Fig. 6a) a current is set up in the crossbar, establishing a field to oppose that of the drive. The geometry (Fig. 4) prevents the net flux from linking the crossbar. The crossbar becomes normally conducting as soon as the induced current reaches its critical value. At this point a portion of the magnetic flux penetrates the crossbar, and the induced supercurrent decays slightly. The crossbar then becomes superconducting inasmuch as the current is now below the critical value. To the extent that the decaying current does not cause significant heating of the crossbar, the above sequence is repeated (saw-tooth area in Fig. 6a) until all the field above the critical level has penetrated the crossbar.

The flux now threads the hole and links the superconductive crossbar. Since with zero resistance the net change of field linking the crossbar must be zero while the applied pulse is being turned off, the induced current begins to decrease. The induced current decreases to zero and then begins to build up in the opposite direction to sustain the flux at a constant value. In the steady-state condition, this current will remain at some constant amplitude as long as the applied current is zero.

If the rise time of the current pulse is decreased (Fig. 6b) the flux penetrates the crossbar more rapidly than is true of the condition described above, apparently accompanied by Joule heating and a rise in temperature. The critical rise time of the material employed was approximately 1000 microseconds. The eddy-current heating seems to lower the critical field as well as to restore more resistance. At this point the process becomes regenerative and the resulting observations can be explained by a temperature rise which is extremely rapid.* The temperature then decreases, as evidenced by the successively increas-

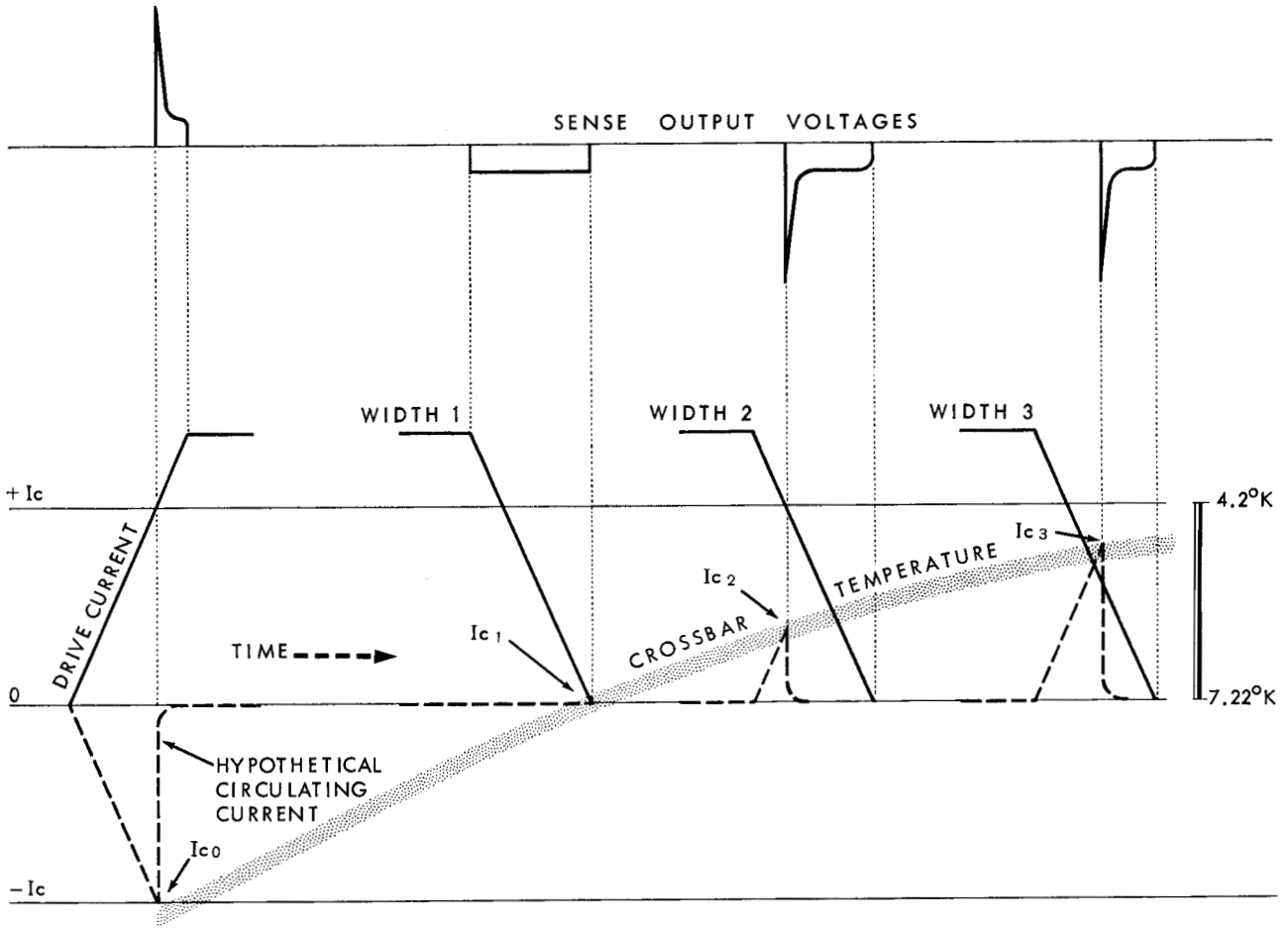

Figure 6c **Characteristic waveforms of test cell.**
Backswing threshold (I_{c1}, I_{c2}, I_{c3}) as function of pulse width. I_c, critical current carrying capacity of the crossbar, increases with decreasing crossbar temperature.

Figure 6d **Characteristic waveforms of test cell.**
Complete memory cycle for fast rise times (sense output voltages are omitted).

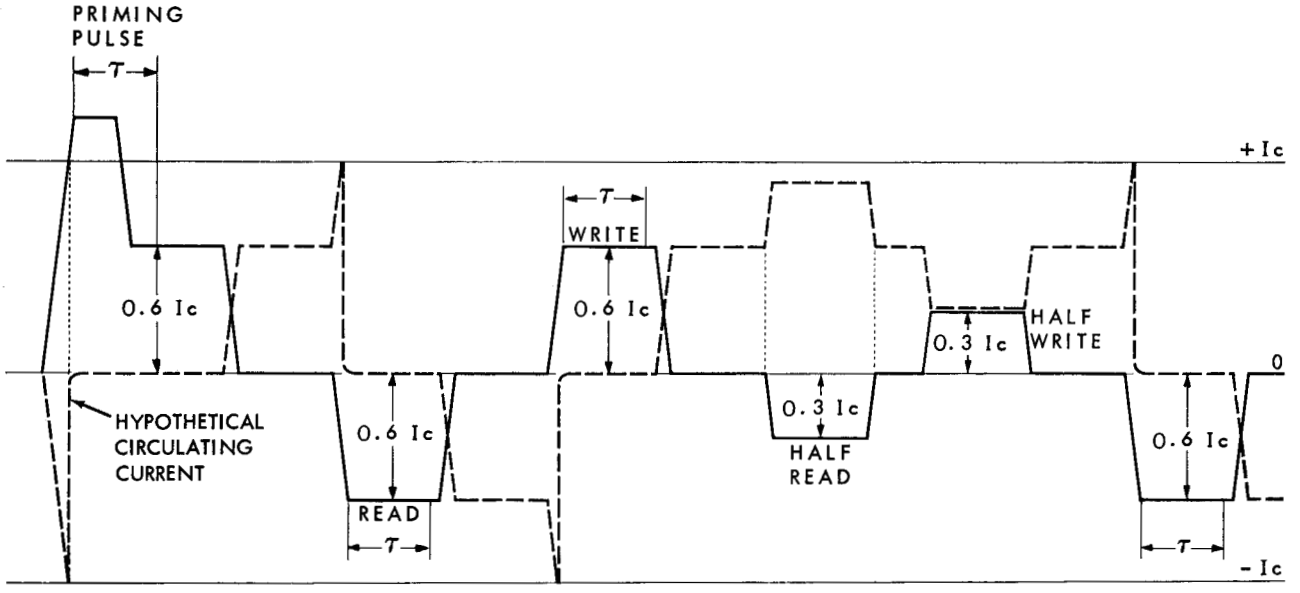

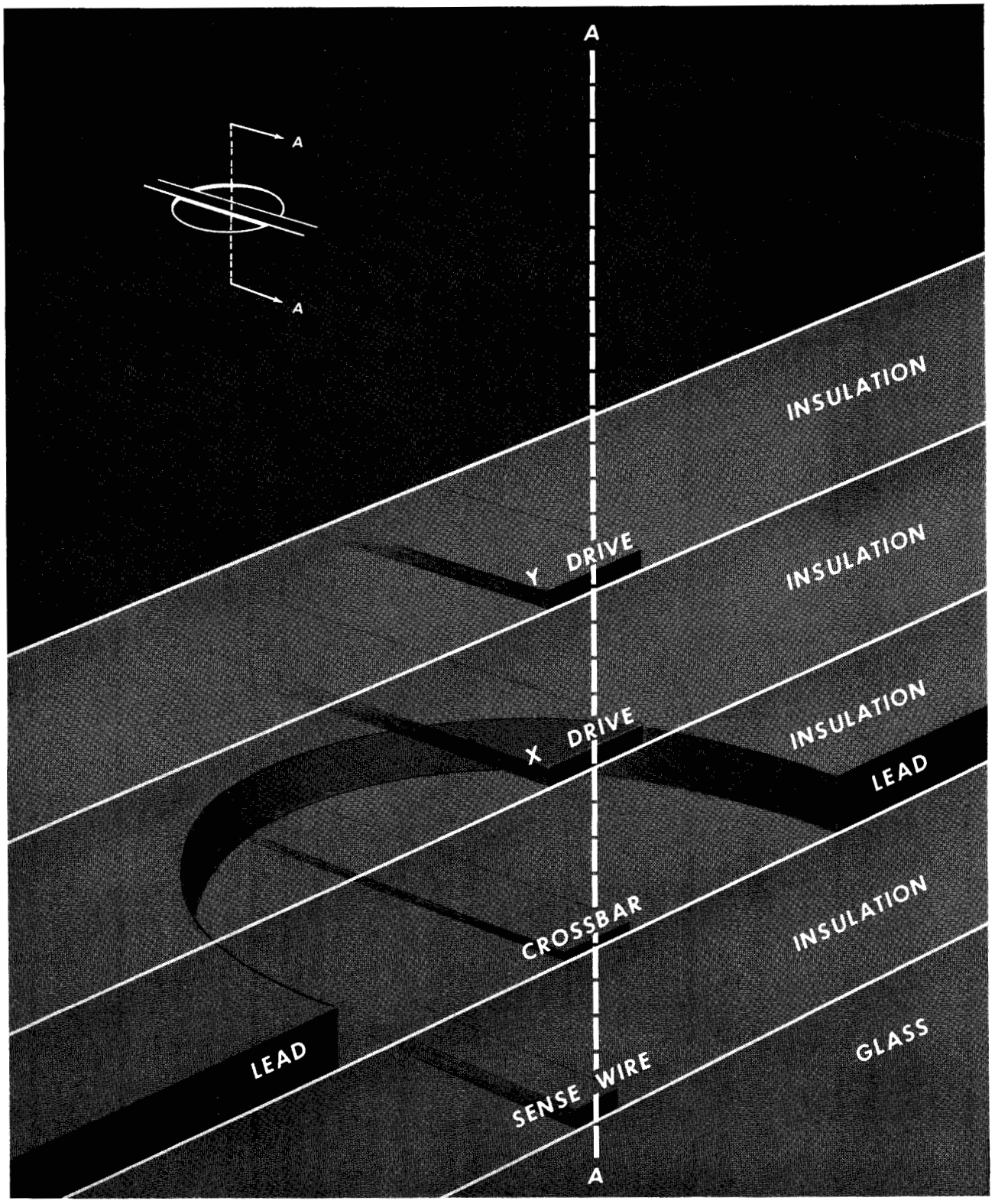

Figure 7 **Above, greatly magnified cross section through center of memory cell; right, actual size of a developmental 4-cell array.**
(The upper illustration is drawn greatly off scale to show layer structure clearly.)

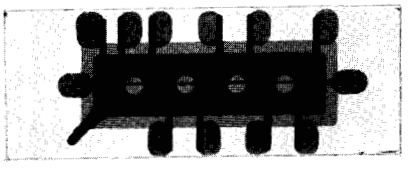

ing values of I_c in Fig. 6c. Mathematically, the loss in energy owing to eddy currents per unit volume is similar to the loss of energy in the magnetic field; hence, assuming an infinitely thick superconductor,

$$\mathcal{E}_e = \frac{H^2 - H_c^2}{8\pi}, \tag{1}$$

where H_c is the critical field for the destruction of the superconducting state. Also, there is a cooling effect owing to the latent heat of the transition of an amount

$$\mathcal{E}_l = \frac{H_c V T}{4\pi} \frac{\partial H_c}{\partial T}. \tag{2}$$

When eddy-current loss exceeds the cooling effect of the latent heat, the temperature begins to rise, and the term H_c^2 in Eq. (1) drops to zero, causing a further increase in the loss by eddy current. However, in the case of the memory cell, an exact solution has not yet been found for the derivation of H, and the peak temperature cannot be determined. From experimental observations, however, we deduce that the temperature rises above T_c, and, in consequence, the resistance of the crossbar is completely restored. When all the flux has penetrated the bar, the temperature in the bar then begins to decrease. Investigations reveal that the time factor for the temperature of the bar to decrease to essentially the ambient is a function of the thickness of the film and the substrate. With silicon monoxide as the insulating material between the drive lines, and with glass as the substrate, and with a film-thickness of 900 A, the drive-current requirement was 300 ma, with a heat-decay time of 0.5 microsecond. The time required to restore the superconducting state of lead-indium films on mica has been measured at less than 0.1 microsecond.

If the drive-current rise time is in the intermediate range (as in Fig. 6b) the relaxation time of less than one microsecond is complete before the current stops rising.† As long as the current continues to rise, the induced current builds up to a maximum, exceeds the threshold, and falls back to zero. The bar then goes superconducting, causing the current to begin to build up again.

The operation of the test memory cell does not depend on slow rising or falling pulses as long as the width of the pulse is greater than the heat relaxation time. In addition the amplitude of the circulating current must be less than the threshold. Exceeding the threshold would cause a heating problem during the fall time, which would destroy the stored information.

Application to computer functions

The switching speed of the developmental-model test memory cell (Figs. 1 and 7) is approximately 0.01 μsec. This speed of operation is about 100 times faster than the ferrite-core memories in present use. The drive-current requirements of the test memory cell are 150 ma, as compared with 400 ma for ferrite-core memories. An important characteristic of the test memory cell is the total absence of delta-noise‡ ordinarily found in core-memory arrays. This extraordinary feature is the natural consequence of a separation of the drive and sense wires by means of a perfectly conducting plane, i.e., the film. An additional advantage of the test memory cell for computer applications is the packaging of the memory cells into extremely small arrays by means of vacuum-metallizing techniques capable of producing film materials with thickness on the order of 900 A. And finally, the test memory cell is capable of operating as a nondestructive memory storage device.

Appendix

The purpose of this section is to define the relation of the magnetic field to the drive-current density and to establish the time dependence of the penetration of a magnetic field in the memory cell. Mathematical analyses pertaining to the test memory cell are considered according to four specific categories: (1) thermodynamic treatment of maximum current densities, (2) the London wave equations,[6] (3) boundary conditions, and (4) summary analysis.

• 1. *Thermodynamic treatment of maximum current densities*

The transition occurs when the energy density at the surface of the superconductor exceeds the quantity

$$\frac{H_c^2}{8\pi}. \tag{3}$$

From thermodynamics,[7] the difference in energy density between the superconducting and normal states may be expressed by the equation

$$f_n - f_s = \tfrac{1}{2} \frac{4\pi\lambda^2 J_c^2}{c^2}. \tag{4}$$

where J_c is the critical current density.

The energy available from the magnetic field is

$$f_n - f_s = \frac{H_c^2}{8\pi}. \tag{5}$$

The current density is related to the magnetic field by the equation

$$J = \frac{cH_c}{4\pi\lambda}. \tag{6}$$

In order to obtain a more exact solution, Equation (6) may be modified to account for extra surface energies in very thin samples. In the case of a flat, thin bar no closed solution of the field according to the London theory has been found to date.

*Test results (Fig. 6c) indicate that the temperature reaches its peak value in not more than 10 millimicroseconds.

†If the rise time is faster than the relaxation time the size of the drive current is inconsequential, since the quantity of stored flux depends on the fall time. If the fall time is less than the relaxation time and the critical current is exceeded, there will be no stored flux.

‡"Delta noise" arises from the difference between the half-select voltages in magnetic-core memories.

• 2. *The London wave equations*

If we now consider the equations for the time dependence of the magnetic field associated with the memory cell of Fig. 4, we may start with London's fundamental equation

$$c \operatorname{curl} \Lambda \mathbf{J} = -\mathbf{H} \tag{7}$$

and Maxwell's equations

$$\operatorname{curl} \mathbf{H} = \frac{4\pi \mathbf{J}}{c} + \frac{\dot{\mathbf{e}}}{c} \qquad \operatorname{div} \mathbf{H} = 0,$$

$$\operatorname{curl} \mathbf{e} = -\frac{\dot{H}}{c} \qquad \operatorname{div} \mathbf{e} = 4\pi\rho. \tag{8}$$

The value Λ in (7) is a constant which is characteristic of the material. It has a value of 10^{-31} sec^2. We assume with London that the total current consists of the effects of the superconducting electrons and the normal conducting electrons

$$\mathbf{J} = \mathbf{J}_s + \mathbf{J}_n. \tag{9}$$

Also

$$\mathbf{J}_n = \sigma \mathbf{e}. \tag{10}$$

London has shown that $\mathbf{e}$ in (8) can be neglected for effects which are much slower than 10^{-12} second, so that

$$\operatorname{div} \mathbf{e} = 0,$$

from Equation (8)

$$\operatorname{div} \mathbf{J} = 0. \tag{11}$$

Carrying out the usual treatment, we eliminate $\mathbf{e}$ and $\mathbf{J}$ and obtain an equation for $\mathbf{H}$:

$$c^2 \nabla^2 \mathbf{H} = \frac{4\pi}{\Lambda} \mathbf{H} + 4\pi\partial\dot{\mathbf{H}} + \ddot{\mathbf{H}}. \tag{12}$$

Equation (12) describes the microscopic field generally, the first term on the right reflects the superconducting effects, the second corresponds to the eddy current and the third the displacement current.

London has shown that the ratios among the three effects of Equation (12) is given by

$$|J_s| : |J_n| : |J_d| = |: \Lambda\partial\omega : \frac{\Lambda\omega^2}{4\pi}. \tag{13}$$

As long as the frequency ω is lower than 10^{12} sec^{-1} the supercurrent contribution is dominant.

When the transition to the normal state occurs, Equation (12) reduces to

$$c^2 \nabla^2 \mathbf{H} = 4\pi\partial\dot{\mathbf{H}}. \tag{14}$$

• 3. *Boundary conditions*

We assume in the geometry of Fig. 4 that the field strength depends only on one spatial dimension X and time T, where X is measured normal to the surface of the film. The magnetic field due to the drive current is assumed to be uniformly distributed across the crossbar.

Cgs units are assumed throughout the following discussion. Equation (14) reduces to

$$H_{xx} = \frac{4\pi\mu H_t}{\rho}. \tag{15}$$

If we postulate another material (air) of thickness D and infinite resistivity placed adjacent to the lead, the field strength in the air will be uniform in space, variable in time and equal to that at the lead interface. At time $t=0$ we apply a constant field H_0 to the lead ($X=0$). The following boundary value problem describes the propagation of the field:

$$H_{xx} = \frac{4\pi\mu H_t}{\rho} \qquad t \geqslant 0 \qquad 0 \geqslant X \geqslant L$$

$$H(0,t) = H_0 \qquad H(X,0) = 0$$

$$H_x(L,t) = -cH_t(L,t). \tag{16}$$

The final condition is a consequence of the conservation of flux through the boundary $X=L$.

$$c = \frac{4\pi D\mu}{\rho}; \tag{17}$$

$$DH(L,t) + \frac{\rho}{4\pi\mu} \int_0^t H_x(L,t)\partial t = 0. \tag{18}$$

To solve the boundary-value problem, first introduce dimensionless parameters as follows:

Let:

$$T = \frac{\rho t}{4\pi\mu L^2}; X = \frac{X}{L}; Q = \frac{D}{L}; h = \frac{H}{H_0}; \tag{19}$$

Then:

$$H_{xx} = h_T. \tag{20}$$

The Laplace transform $\bar{h}(20)$ is

$$H_{xx}(X,s) = s\bar{h}(X,s); \tag{21}$$

$$\bar{h}(0,s) = \frac{1}{s}; \bar{h}_x(1,s) = -Qs\bar{h}(1,s). \tag{22}$$

This reduces the problem to one in ordinary differential equations whose solution is easily verified to be:

$$\bar{h}(X,s) = \frac{1}{s}\left\{\frac{Q\sqrt{s}\sinh\sqrt{s}(1-X) + \cosh\sqrt{s}(1-X)}{Q\sqrt{s}\sinh\sqrt{s} + \cosh\sqrt{s}}\right\}. \tag{23}$$

The inverse Laplace transformation of $\bar{h}(X,s)$ is obtained by an integration in the complex plane.[8] In our case this problem reduces to a summation involving the residues of $\bar{h}(X,s)$ in a right-half plane:

$$h(X,T) = 1 - 2\sum_{k=1}^{\infty} \frac{\sin\gamma_k X \exp(-\gamma_k^2 T)}{\gamma_k(1+Q\sin^2\gamma_k)}, \tag{24}$$

where the γ_k are roots of:

$$\tan\gamma = \frac{1}{Q\gamma}. \tag{25}$$

Reverting to the original variables, we have

$$H(X,t)=H_0\left\{1-2\sum_{h=1}^{\infty}\frac{\sin\gamma_h\,\frac{X}{L}\exp\left(\frac{-\gamma_h^2\rho t}{4\pi\mu L^2}\right)}{\gamma_h\{1+\rho\sin^2\gamma_h\}}\right\}. \quad (26)$$

As we shall see, the values of ρ that interest us are large enough so that the first eigenvalue can be approximated $\gamma_1=\frac{1}{\sqrt{Q}}$. Furthermore, the coefficient of $\exp(-\gamma_h^2 T)$ is always less than unity and the values of γ_h for $h>1$ are larger than $\pi/2$, enabling us to disregard all terms after the first. The field strength at $X=L$ becomes:

$$\frac{H(L,t)}{H_0}=1-\exp\left(\frac{-\rho t}{4\pi\mu L^2 Q}\right). \quad (27)$$

Setting H/H_0 equal to $1-1/e$ determines "t_e", which is the time required for the output voltage to reach $1/e$ of its peak value

$$t_e=\frac{4\pi L^2 Q\mu}{\rho}=\frac{4\pi LD\mu}{\rho}. \quad (28)$$

- 4. *Summary analysis*

Assuming a value of one microhm-centimeter for the resistivity of lead at 4.2°K, a thickness of 1000 A for the film, and a hole diameter of 0.3 cm, the relaxation time can be calculated as 12.5×10^{-9} sec. The uncertainty as to the resistivity could account for an order of magnitude error in the above calculations. Nevertheless, the agreement between the observed and calculated times is sufficient to indicate the probable validity of the assumption.

Acknowledgments

The author wishes to express gratitude to Dr. R. L. Garwin, Dr. D. R. Young and to C. J. Kraus and his group for many valuable discussions and criticisms of this program. Thanks are due also to O. Reuhr for his assistance and the mathematical analysis he provided.

References

1. Onnes, H. K., *Commun. Phys.*, Lab. Univ. Leiden No. 119b (1911).
2. Buck, D. A., "The Cryotron—A Superconductive Computer Component," *Proceedings of the IRE* **44,** No. 4, 482-493 (April 1956).
3. Collins, S. C., private communication.
4. Laue, M. Von, *Theory of Superconductivity,* Academic Press Inc., New York, 1952.
5. Alers, P. B., "Structure of the Intermediate State of Superconducting Lead," *Phys. Rev.* **105,** 104-108 (Jan. 1, 1957).
6. London, F., *Superfluids,* John Wiley and Sons Inc., New York, 1954, Vol. 1.
7. Shoenberg, D., *Superconductivity,* Cambridge University Press, 1952.
8. Churchill, R. V., *Modern Operational Mathematics in Engineering,* McGraw-Hill, 1944, Chap. VI.

List of symbols

c = Velocity of light
C = Constant related to properties of dielectric material
D = Diameter of fringing of magnetic flux lines
πD = Diameter of hole in hard superconducting film
$\mathcal{E}_c$ = Energy loss at critical field strength
$\mathcal{E}_i$ = Energy of latent heat of transition
e = Electric field vector
f_s = Free-energy density of the superconducting state
f_n = Free-energy density of the normal state
H = Magnetic field
H_c = Critical field
H_0 = Initial field
H_t = $\partial H/\partial t$
I_c = Critical current-carrying capacity of crossbar
I_{ind} = Hypothetical induced current in crossbar and film
J = Current density
J_c = Critical current density
J_n = Density of normal electrons
J_s = Density of superelectrons
L = Thickness of film
λ = Penetration depth
Λ = London constant (10^{-31} sec^2)
μ = Permeability
ω = $2\pi f$
ρ = Resistivity
σ = Conductivity
t = Time
τ = Heat relaxation time

Received June 4, 1957